Influence of Atlantic meridional overturning circulation on the East Asian winter monsoon

Youbin Sun[1]*, Steven C. Clemens[2], Carrie Morrill[3], Xiaopei Lin[4], Xulong Wang[1] and Zhisheng An[1]

The last glacial period was characterized by abrupt, millennial-scale climate change. These climate fluctuations are particularly pronounced in records of the East Asian monsoon system[1-8], and seem to be linked to changes in North Atlantic circulation. Here we present records of grain size variations from the northwestern Chinese Loess Plateau, dated using optically stimulated luminescence. We reconstruct changes in the strength of the East Asian winter monsoon over the past 60,000 years and find reconstructed millennial-scale variations that are broadly correlated with temperature variations over Greenland, suggesting a common forcing. We investigate the effect of a slow-down of Atlantic meridional overturning circulation on the monsoon system using a coupled climate model simulation with added freshwater flux into the northern North Atlantic, and find a strengthening winter monsoon circulation over the regions that supply dust to the Loess Plateau and a reduction in summer monsoon precipitation over East Asia. We conclude that Atlantic meridional overturning circulation is a driver of abrupt change in the East Asian winter and summer monsoon systems, and that the northern westerlies play a role in transmitting this signal from the North Atlantic to the Asian monsoon regions.

Interactions between the tropics and high latitudes play a key role in the inter- and intra-hemispheric coupling of abrupt climate change. Greenland temperature, as an indication of high-latitude climate[9,10], is largely dependent on the Atlantic meridional overturning circulation (AMOC; refs 11,12). By contrast, the Asian summer monsoon, a low-latitude process, is dynamically linked to the migration of the Intertropical Convergence Zone[13-15]. Similarity of glacial millennial-scale climate variability recorded by Chinese speleothems[4] and Greenland ice cores[9,10] implies a plausible influence of high-latitude northern hemisphere climate on East Asian monsoon circulation[16,17], although tropical processes have also been implicated as possible drivers of millennial-scale climate change[18]. Changes in the westerly jet and the Siberian–Mongolian High were previously considered as a mechanism linking abrupt climate changes in the North Atlantic and East Asia[1-5,7,19-21]. The remote impacts of the North Atlantic climate change on the wind and precipitation variability in East Asia can be further assessed by integrating palaeoclimate proxy data and model simulations.

Unlike the African and Indian monsoons, the East Asian monsoon contains a unique mid-latitude component (a strong winter monsoon), which is characterized by prevailing low-level northwesterly winds associated with the Siberian–Mongolian High[22]. The winter monsoon encompasses a larger meridional domain than the summer monsoon and can act as a medium to transmit climate signals from the high-latitude North Atlantic to the mid- and low-latitude regions[1,3,6,7]. Thus, reconstruction of past winter monsoon fluctuations is key to deciphering the hemispheric coupling between abrupt climate changes in the North Atlantic and East Asia. Here we report closely spaced optically stimulated luminescence (OSL) ages for two loess sequences in the northwestern Chinese Loess Plateau, yielding an independent chronology for assessing rapid winter monsoon shifts and a robust assessment of the coupling between Greenland temperature and East Asian monsoon variability. Furthermore, an integration of loess, speleothem and ice-core records with model simulations tests hypotheses about the dynamical causes of rapid climate changes.

Loess sequences at Jingyuan (36.35° N, 104.6° E, 2,210 m above sea level) and Gulang (37.49° N, 102.88° E, 2,400 m above sea level) are situated in the depocentre of modern dust storms[23], at distances of 80 km and 10 km, respectively, from the modern Tengger Desert margin (Fig. 1). Mean annual precipitation over the past 55 years is 233 mm at Jingyuan and 164 mm at Gulang, with 55% of the annual precipitation falling during the summer season. Two 20-m sampling pits were excavated at Jingyuan and Gulang. Forty OSL ages were used to generate an independent loess chronology, indicating that the 20-m loess sequences at Jingyuan and Gulang accumulated over the past 48 and 60 kyr, respectively (Methods, Supplementary Note S1, Tables S1 and S2, and Figs S1–S5). High sedimentation rates (10–130 cm kyr^{-1} at Jingyuan and 9–63 cm kyr^{-1} at Gulang; Supplementary Fig. S6) and weak pedogenesis make these two loess sequences sensitive recorders of rapid monsoon changes.

We argue that the grain size of the loess samples at Gulang and Jingyuan mainly reflects changes in winter monsoon strength[24] (Supplementary Note S2). The Gulang and Jingyuan grain size records indicate distinct millennial-scale and glacial–interglacial variability (Fig. 2). Gulang grain size shows higher amplitude and more abrupt transitions, yielding a well-resolved record of millennial-scale winter monsoon fluctuations. Relatively high accumulation rates and coarser grain size characterize the Jingyuan section (Supplementary Fig. S6), a result of its proximity to the Yellow River (a likely local dust source). Significant dust contribution from this local source may attenuate the abrupt grain size changes recorded in the Jingyuan loess section. Our OSL-dated records indicate, with certain exceptions, that rapid grain size oscillations are aligned with Heinrich and Dansgaard–Oeschger (DO) events recorded in the North Greenland ice core (NGRIP; refs 10,25,26) and Chinese speleothems[4,27,28] (Fig. 2).

[1]State Key Laboratory of Loess and Quaternary Geology, Institute of Earth Environment, Chinese Academy of Sciences, Xi'an 710075, China, [2]Department of Geology, Brown University, Providence, Rhode Island 02912-1846, USA, [3]Cooperative Institute for Research in Environmental Sciences (CIRES), University of Colorado at Boulder, and NOAA's National Climatic Data Center, Boulder, Colorado 80305-3328, USA, [4]Physical Oceanography Laboratory, Ocean University of China, Qingdao 266100, China. *e-mail: sunyb@ieecas.cn.
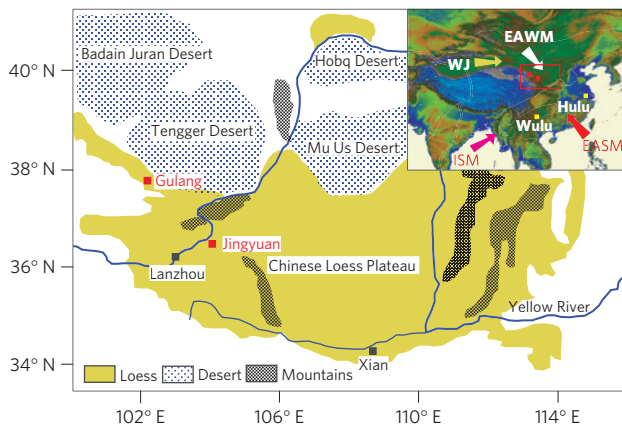
Figure 1 | Site location and atmospheric circulation. Major atmospheric circulation regimes in East Asia and locations of Gulang and Jingyuan loess profiles as well as Hulu and Wulu caves. ISM-Indian summer monsoon, EASM-East Asian summer monsoon, EAWM-East Asian winter monsoon, WJ-Westerly jet.

Coarsening of mean grain size around 16, 24, 30, 39, 48 and 55 kyr indicates that the North Atlantic Heinrich events (H_1–H_{5a}) are associated with strong winter monsoon circulation in the Chinese Loess Plateau, although the timing and amplitude of coarsening grain size around 24 and 30 kyr at the Gulang section are slightly mismatched relative to the H_2 and H_3 events. Many of the millennial-scale events (DO 7–17, 34–60 kyr) are well aligned among the loess, speleothem and ice-core records, showing similar amplitudes and durations as well (Fig. 2). A remarkable grain size event is present between DO 14 and 15, which is absent in the Hulu speleothem record but distinct in the NGRIP (ref. 10) and Wulu records[28]. The validity of the OSL chronology is strongly supported by the good correlation between loess grain size and radiometrically dated speleothem δ^{18}O across events from DO 7 to DO 17. The correlative nature of these DO

events in the ice-core, loess and cave records (all on independent chronologies) directly links Heinrich- and DO-scale variability in the Loess Plateau to that in Greenland and eastern China over the interval 34–60 kyr.

In contrast, DO events in the interval 20–34 kyr are not as well correlated among the three records, indicating different amplitudes, numbers of resolved events and event durations. Within this interval the Gulang grain size record indicates thirteen distinct events (labelled 'a' to 'm'). Neither the cave nor the ice-core records indicate thirteen events within this interval. Three exceptionally strong events (a, b and c) between 20 and 23 kyr in the Gulang record have no counterparts in the NGRIP or cave records. However, these large amplitude oscillations are clearly expressed as heavy-isotope events in Guliya ice-core δ^{18}O on the Tibetan Plateau[8]. The OSL age model suggests that events d, i, l and m are most proximal to DO 2, 4, 5 and 6 in the cave records[4,27], although we acknowledge that other correlations are possible within the OSL age error (for example, grain size event k to DO 5, and events l and m to DO 6; Fig. 2).

Clear differences in resolution exist between the loess grain size, ice-core and speleothem records. For example, the Gulang grain size data show three distinct fine-scale oscillations within DO 8, four within DO 12 and six within DO 14. This centennial-scale variability is not clearly expressed in either the speleothem or ice-core records. Replication of these structures in proximal Gulang sites will be required to test for reproducibility. Different expression of these abrupt events in NGRIP δ^{18}O, loess grain size, and speleothem δ^{18}O records indicates that these palaeo-proxies document different aspects (temperature, wind and precipitation) of the climate response in three different regions (Greenland, Chinese Loess Plateau and eastern China). Similar regional differences also exist within the Chinese Loess Plateau, possibly due either to age model discrepancies, or to the resolution and continuity of the loess sequences[1–3,29,30].

The DO-scale variability common to Greenland ice cores, loess and cave records, particularly within the interval 34–60 kyr, is plausibly linked to rapid AMOC oscillations[11,12]. Both geological
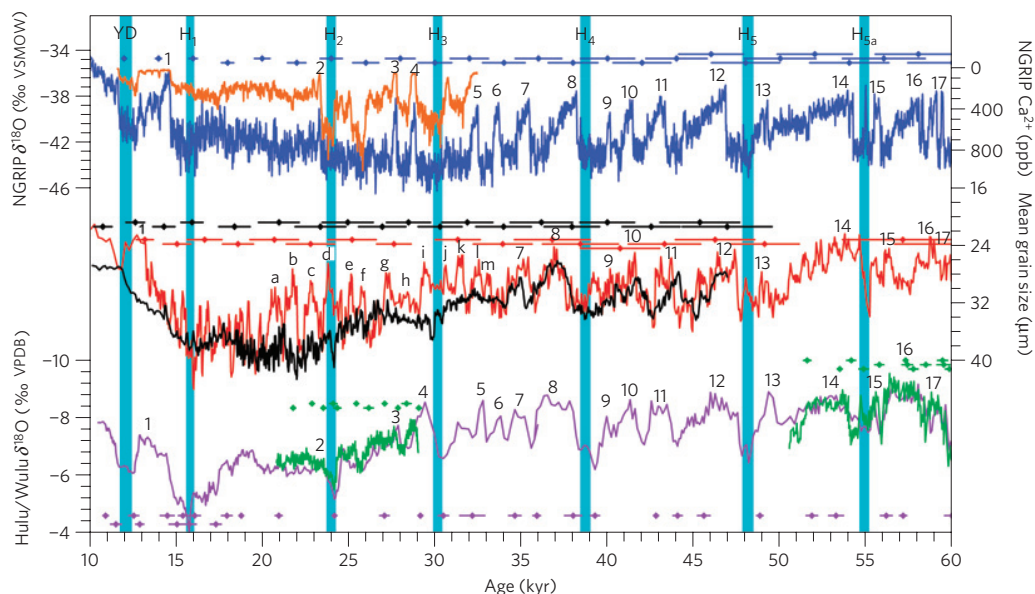

Figure 2 | Monsoonal and North Atlantic climate records. Comparison of Gulang (red) and Jingyuan (black) mean grain size with NGRIP δ^{18}O (blue) and Ca^{2+} (orange) records[10,25,26] and Hulu(purple)/Wulu(green) speleothems[4,27,28]. Sky-blue bars denote the Heinrich-like events identified in the three records. Black numbers (7–17, 34–60 kyr) denote well aligned DO events identified in the three records. Over the interval 20–34 kyr the Gulang grain size record indicates thirteen distinct events (labelled 'a' to 'm'). OSL ages and errors (1σ error bars) of two loess sequences are marked on the grain size curves. The ^{230}Th ages and errors (2σ error bars) are shown on the speleothem records. Age errors for the NGRIP ice core are the maximum counting errors on the Greenland Ice Core Chronology 2005 (GICC05) timescale.

evidence and modelling results suggest that rapid climate change in the North Atlantic region (for example, Heinrich and DO events) can result in variability in the strength and position of the westerly jet, influencing northern hemisphere climate, including East Asia[1–3,7,19–21]. Considering a North Atlantic origin of abrupt climate change, one would expect a distinct response in monsoonal wind and precipitation variability in East Asia. Monsoonal proxy results do indicate that significant strengthening of the winter monsoon and weakening of the summer monsoon are associated with strong cooling in the North Atlantic. North Atlantic water-hosing experiments using the Community Climate System Model version 3 (CCSM3) under Last Glacial Maximum (LGM) boundary conditions also suggest a coupled response of the winter and summer monsoons to reductions of the AMOC (Methods and Supplementary Note S3).

In the water-hosing experiments, the AMOC weakens from a control mean of 16.8 Sv to a mean of 5.6 Sv (here Sv stands for Sverdrup; $1\,\mathrm{Sv} = 10^6\,\mathrm{m}^3\,\mathrm{s}^{-1}$) after 50 years (Supplementary Note S3 and Fig. S7). Climate in most parts of the Northern Hemisphere, including Greenland, responds in a matter of decades or less. As AMOC slows, global northward ocean heat transport is reduced at all latitudes, including a ~60% reduction north of 40° N. This is partially, but not completely, offset by an increase in atmospheric heat transport. Consequently, temperatures in the northern hemisphere decrease, with the largest cooling during the winter associated with areas of sea-ice expansion in both the North Pacific and North Atlantic (Supplementary Note S3 and Fig. S8). The increase in the meridional (latitudinal) temperature gradient leads to stronger westerly winds in the mid-latitudes and strengthened winter wind speed above the northwestern Chinese Loess Plateau and the major Asian dust source regions (Fig. 3a). Both surface winter wind stress, which is key for dust entrainment and transportation, as well as 750 mb wind speed (westerly), which is important for long-range dust transport, significantly increase in the hosing experiment.

Following hosing, there is a decrease in the summer precipitation in East Asia (Fig. 3b), which today is associated with moisture convergence along the Meiyu front[22]. Cyclonic circulation anomalies associated with a weakening of the subtropical high probably reduced southwesterly moisture transport and moisture convergence to the Meiyu front. Furthermore, an overall reduction in specific humidity caused by colder temperatures dries the northern hemisphere atmosphere (Supplementary Table S3). Many of our modelled summer circulation anomalies are consistent with results from a pre-industrial hosing experiment[17], indicating that similar atmospheric and oceanic responses to hosing were probably in operation during the last glacial. In that simulation, cooling in the North Atlantic associated with the reduction of the AMOC causes a southward shift of the Intertropical Convergence Zone in both the Atlantic and the Pacific, a strengthening of the Walker circulation in the northern tropical Pacific, and a weakening of the East Asian summer monsoon[17].

A robust comparison of loess grain size with Chinese speleothem and Greenland ice-core records indicates that Greenland temperature and EAM variability are coupled on millennial timescales during the interval 34–60 kyr. North Atlantic water-hosing experiments suggest a dynamical response of the monsoonal wind and precipitation in East Asia to a reduction of the AMOC. Freshwater forcing results in an increased latitudinal temperature gradient and strong winter winds throughout much of the atmosphere in the Northern Hemisphere mid-latitudes. Meanwhile, the North Pacific subtropical high weakens following the hosing and the resulting strong cyclonic circulation anomaly leads to reduced convergence along the Meiyu front in East Asia and decreased summer precipitation surrounding Hulu Cave. Integration of these modelling results
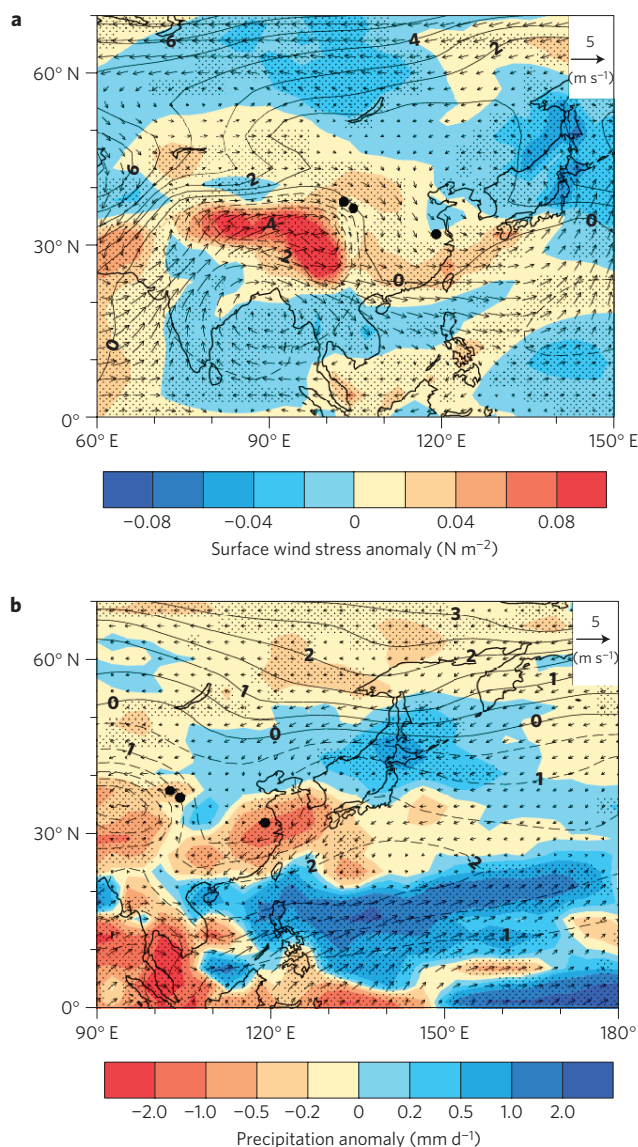

Figure 3 | CCSM3 simulated surface wind stress and precipitation anomalies between the water-hosing experiment and the glacial control simulation. a, Boreal winter (December–February) surface wind stress ($\mathrm{N\,m^{-2}}$, colour), sea-level pressure (hPa, lines) and 750 mb wind vectors ($\mathrm{m\,s^{-1}}$). **b**, Boreal summer (July–August) precipitation ($\mathrm{mm\,d^{-1}}$, colour), sea-level pressure (hPa, lines) and wind vectors from the lowest atmospheric model level ($\mathrm{m\,s^{-1}}$). Stippling shows areas of statistically-significant differences in surface wind stress and precipitation at the 95% level according to a Student's t-test. Black dots show locations of Gulang, Jingyuan and Hulu discussed in text.

and our palaeoclimate data reveals that reduction of the AMOC probably played a key role in driving abrupt monsoon changes in East Asia.

Methods

We took 2000 powder samples at 2-cm intervals from these two 20-m loess pits. Grain size distribution of the samples was measured using a Malvern 2000 laser instrument after removal of organic matter and carbonate. Samples for OSL dating were collected in stainless tubes hammered into a freshly-cleaned section face, and then wrapped in aluminium foil until processing under subdued red light in the luminescence dating laboratory of the Institute of Earth Environment, Chinese Academy of Sciences. Material from both ends of the sample tubes was excluded from equivalent dose (ED) estimation and was used for radioisotope measurements to obtain the environmental dose rate. Samples were pretreated with 30% HCl and 10% H_2O_2 to remove the carbonates and organic matter, respectively. Then the

50–90 µm fractions were isolated by sieving and etched with HF (40%) for 60 min. The purity of the isolated quartz was checked by infrared stimulation, and in the single aliquot regenerative-dose (SAR) dating protocol a further infrared bleaching (Step 3 and 7, Supplementary Table S1) was also applied to further remove any signal from potential feldspar contamination.

All OSL measurements were performed using a Daybreak 2200 automated OSL reader equipped with a combined blue (470 ± 5 nm) and infrared (880 ± 80 nm) LED OSL unit, and a ^{90}Sr/^{90}Y beta source (0.107 Gy/s) for irradiations. All luminescence measurements were made at 125 °C for 200 s with both infrared and blue stimulation powers, nominally at ~45 mW cm^{-2}. Luminescence emissions were detected by an EMI 9235QA photomultiplier tube with two 3 mm thick U-340 glass filters. Forty-four OSL dates were estimated using a single-aliquot regenerative-dose protocol (Supplementary Table S2 and Fig. S3). After application of a three-point smoothing fit to the OSL dates (excluding four age inversions), chronologies of the Jingyuan and Gulang sections were generated by linear interpolation between forty smoothed OSL dates (Supplementary Note S1 and Fig. S4). This OSL chronology is independent of any underlying assumptions linking loess proxies to a particular climate forcing mechanism.

We use CCSM3 to simulate climate changes associated with North Atlantic freshwater forcing during the LGM (Supplementary Note S3). CCSM3 is a global, ocean–atmosphere–sea-ice–land-surface climate model coupled without flux corrections. The atmospheric component is the Community Atmosphere Model version 3 at a horizontal resolution of T42 (approximately 2.8° in latitude and longitude) and 26 hybrid vertical levels. The land model, which includes river routing and prescribed plant functional types, uses the same grid as the atmospheric component. The ocean model is an implementation of the Parallel Ocean Program model with a nominal grid spacing of approximately 1° in latitude and longitude, and greater resolution in the tropics and North Atlantic. The vertical resolution is 40 levels, extending to a depth of 5.5 km. The dynamic-thermodynamic sea-ice model uses the same horizontal grid and land mask as the ocean component.

We used a control simulation with boundary conditions appropriate for 21 kyr, as defined by the Paleoclimate Modelling Intercomparison Project Phase 2 (Supplementary Note S3 and Fig. S9). In the water-hosing experiment, which was branched from the control simulation, 1 Sverdrup (10^6 m^3 s^{-1}) of freshwater was applied as a virtual negative salinity flux to the North Atlantic between 50° and 70° N. Freshwater was added for 100 years, starting at year 400 of the LGM simulation. The total volume of water introduced to the North Atlantic over the 100-year period is equivalent to a 9 m sea-level rise. The hosing simulation was designed as a sensitivity experiment to examine physical processes and is not meant to exactly replicate past events. In this study, we analysed the last 50 years of the hosing experiment compared against 50 years of the control simulation.

References

1. Porter, S. C. & An, Z. S. Correlation between climate events in the North-Atlantic and China during last glaciation. *Nature* **375,** 305–308 (1995).
2. Guo, Z. T. *et al*. High frequency pulses of East Asia monsoon climate in the last two glaciations: Link with the North Atlantic. *Clim. Dyn.* **12,** 701–709 (1996).
3. Ding, Z. L. *et al*. Correlation of Dansggard–Oeschger cycles between Greenland ice and Chinese loess. *Paleoclimates* **4,** 28l–29l (1998).
4. Wang, Y. J. *et al*. A high-resolution absolute-dated late Pleistocene monsoon record from Hulu Cave, China. *Science* **294,** 2345–2348 (2001).
5. Tada, R., Irino, T. & Koizumi, I. Land–ocean linkage in orbital and millennial timescales recorded in Late Quaternary sediments of the Japan Sea. *Paleoceanography* **14,** 236–247 (1999).
6. Oppo, D. W. & Sun, Y. B. Amplitude and timing of sea-surface temperature change in the northern South China Sea: Dynamic link to the East Asian monsoon. *Geology* **33,** 785–788 (2005).
7. Nagashima, K. *et al*. Millennial-scale oscillations of the westerly jet path during the last glacial period. *J. Asian Earth Sci.* **40,** 1214–1220 (2011).
8. Thompson, L. G. *et al*. Tropical climate instability: The last glacial cycle from a Qinghai–Tibetan ice core. *Science* **276,** 1821–1825 (1997).
9. Dansgaard, W. *et al*. Evidence for general instability of past climate from a 250-kyr ice-core record. *Nature* **364,** 218–220 (1993).
10. North Greenland Ice Core Project (NGRIP) members, High-resolution record of Northern Hemisphere climate extending into the last interglacial period. *Nature* **431,** 147–151 (2004).
11. Bond, G. *et al*. Correlations between climate records from North Atlantic sediments and Greeland ice. *Nature* **365,** 143–147 (1993).
12. Liu, Z. *et al*. Simulation of last deglaciation with a new mechanism for Bølling–Allerød warming. *Science* **325,** 310–314 (2009).
13. Webster, P. J. *et al*. Monsoons: Processes, predictability, and the prospects for prediction. *J. Geophys. Res.* **103,** 14451–14510 (1998).
14. Chao, W. C. & Chen, B. The origin of monsoons. *J. Atmos. Sci.* **58,** 3497–3507 (2001).
15. Yancheva, G. *et al*. Influence of the intertropical convergence zone on the East Asian monsoon. *Nature* **445,** 74–77 (2007).
16. Rohling, E. J., Mayewski, P. A. & Challenor, P. On the timing and mechanism of millennial-scale climate variability during the last glacial cycle. *Clim. Dyn.* **20,** 257–267 (2003).
17. Zhang, R. & Delworth, D. L. Simulated tropical response to a substantial weakening of the Atlantic thermohaline circulation. *J. Clim.* **18,** 1853–1860 (2005).
18. Clement, A. C. & Peterson, L. C. Mechanisms of abrupt climate change of the last glacial period. *Rev. Geophys.* **46,** RG4002 (2008).
19. Yanase, W. & Abe-Ouchi, A. The LGM surface climate and atmospheric circulation over East Asia and the North Pacific in the PMIP2 coupled model simulations. *Clim. Past* **3,** 439–451 (2007).
20. Jin, L., Chen, F., Ganopolski, A. & Claussen, M. Response of East Asian climate to Dansgaard/Oeschger and Heinrich events in a coupled model of intermediate complexity. *J. Geophys. Res.* **112,** D06117 (2007).
21. Wu, L., Li, C. & Yang, C. Global teleconnections in response to a shutdown of the Atlantic meridional overturning circulation. *J. Clim.* **21,** 3002–3019 (2008).
22. Ding, Y. H. *Monsoons Over China* (Kluwer Academic Publisher, 1994).
23. Sun, J. M., Zhang, M. Y. & Liu, T. S. Spatial and temporal characteristics of dust storms in China and its surrounding regions, 1960–1999: Relations to source area and climate. *J. Geophys. Res.* **106,** 18325–18333 (2001).
24. An, Z. S., Kukla, G., Porter, S. C. & Xiao, J. L. Late Quaternary dust flow on the Chinese Loess Plateau. *Catena* **18,** 125–132 (1991).
25. Rasmussen, S. O. *et al*. Synchronization of the NGRIP, GRIP, and GISP2 ice cores across MIS 2 and palaeoclimatic implications. *Quat. Sci. Rev.* **27,** 18–28 (2008).
26. Svensson, A. *et al*. A 60,000 year Greenland stratigraphic ice core chronology. *Clim. Past* **4,** 47–57 (2008).
27. Zhao, K., Wang, Y. J., Edwards, R. L., Cheng, H. & Liu, D. B. High-resolution stalagmite δ^{18}O records of Asian monsoon changes in central and southern China spanning the MIS 3/2 transition. *Earth Planet. Sci. Lett.* **298,** 191–198 (2010).
28. Liu, D. B. *et al*. Sub-millennial variability of Asian monsoon intensity during the early MIS 3 and its analogue to the ice age terminations. *Quat. Sci. Rev.* **29,** 1107–1115 (2010).
29. Stevens, T., Lu, H. Y., Thomas, D. S. G. & Armitage, S. J. Optical dating of abrupt shifts in the late Pleistocene East Asian monsoon. *Geology* **36,** 415–418 (2008).
30. Sun, Y. B., Wang, X. L, Liu, Q. S. & Clemens, S. C. Impacts of post-depositional processes on rapid monsoon signals recorded by the last glacial loess deposits of northern China. *Earth Planet. Sci. Lett.* **289,** 171–179 (2010).

Author contributions

Y.S. designed the study, performed the fieldwork and grain size analysis, and led the writing of the paper. S.C. contributed to data analysis, interpretation and paper writing. Both C.M. and X.L. analysed the water-hosing experiments. X.W. conducted the OSL dating. All authors contributed to discussion, interpretation of the results and writing of the manuscript.

Additional information

The authors declare no competing financial interests. Supplementary information accompanies this paper on www.nature.com/naturegeoscience. Reprints and permissions information is available online at http://www.nature.com/reprints. Correspondence and requests for materials should be addressed to Y.S.